The 19th NEXT Workshop
ROHM Plaza, Kyoto University Katsura Campus
2013-08-29

Linear Analysis of Energetic-Particle-Driven Low-Frequency Eigenmodes

A. Fukuyama

Department of Nuclear Engineering, Kyoto University, Kyoto, Japan

Outline

- **Full wave approach of linear stability analysis**
- **Full wave code**: TASK/WM
- **Analysis of Alfvén eigenmodes**
  - TAE
  - EPM
  - TAE in rotating plasmas
  - RSAE
- **Progress in full wave analysis**
- **Summary**

Full Wave Approach of Linear Stability Analysis

- **Conventional analysis of global stability analysis**
  - **MHD Analysis** (Ideal, Resistive)
  - **Extended MHD Analysis** (Hall, Multi-fluid)
  - **MHD including Kinetic Effect** (perturbative)
    - Eigen function from MHD analysis
    - Growth rate including kinetic effects
- **Issues in MHD analysis**
  - Propagation in vacuum
  - Strongly coupled with plasma model
- **Full wave approach to global stability analysis**
  - Boundary value problem of Maxwell's equation
  - Dielectric tensor describes plasma response
  - Physical damping mechanism

Damping Mechanism of Alfvén Eigenmodes

- **MHD model**
  - Absorption near Alfvén resonance
    (**Continuous spectrum damping**)
- **Perturbative treatment of kinetic Alfvén waves**
  (**Eigen function: MHD, Damping: Kinetic**)
  - Radiative damping
    (**power propagating outward**)
  - Landau damping
    (**Estimation of parallel wave electric field**)
- **Kinetic absorption mechanism**
  - Electron Landau damping
  - Landau damping of energetic ions

Present Structure of Integrated Modeling Code TASK

- **Integrated code for the analysis of toroidal plasmas**

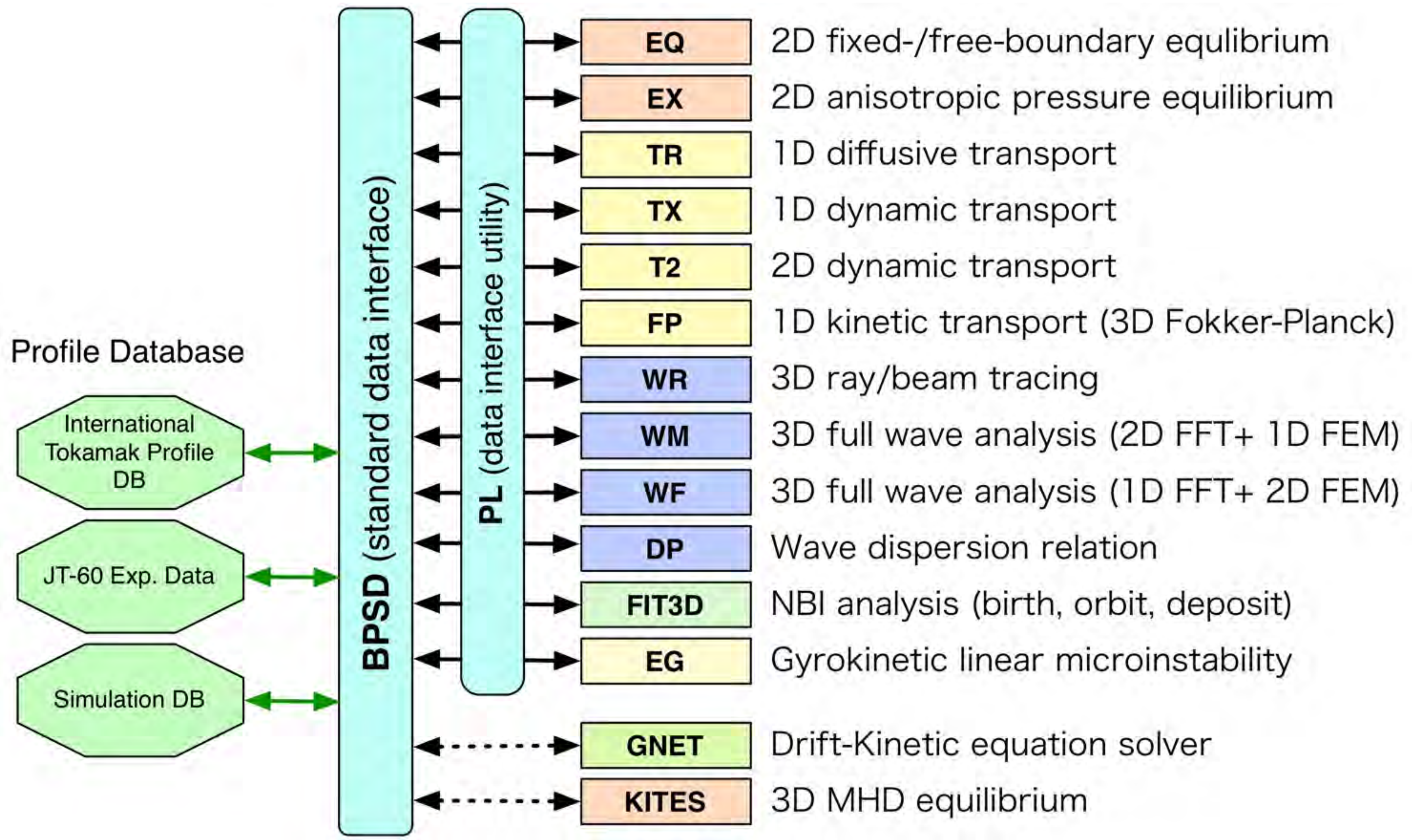

Full wave code in TASK

- **Features of full wave component**: **TASK/WM**
  - Boundary value problem of Maxwell's equation
  - Various models of dielectric tensor: **TASK/DP**
  - Magnetic surface coordinates from MHD Equilibrium Analysis
  - Fourier mode expansion in poloidal and toroidal direction
  - Finite difference method in radial direction
  - Complex wave frequency to maximize the wave field.
- **Other full wave components**
  - Using finite element method
- **Coupling with Fokker-Planck analysis of $f(v)$**: **TASK/FP**
  - Generation of energetic particles

TASK/WM

- **Magnetic surface coordinates**: (ψ, θ, φ)
  - **Non-orthogonal system** (including 3D helical configuration)
- **Maxwell's equation** for stationary wave electric field $\boldsymbol{E}$

$$\nabla \times \nabla \times \boldsymbol{E} = \frac{\omega^2}{c^2} \overleftrightarrow{\epsilon} \cdot \boldsymbol{E} + \mathrm{i}\, \omega \mu_0 \, \boldsymbol{j}_{\mathrm{ext}}$$

  - $\overleftrightarrow{\epsilon}$ **: Dielectric tensor with kinetic effects**: $Z[(\omega - n\omega_{\mathrm{c}})/k_{\parallel}]$
- **Fourier expansion** in poloidal and toroidal directions
  - **Exact parallel wave number**: $k_{\parallel}^{m,n} = (mB^{\theta} + nB^{\varphi})/B$
- **Destabilization by energetic ions** included in $\overleftrightarrow{\epsilon}$
  - **Drift kinetic equation**

$$\left[\frac{\partial}{\partial t} + v_{\parallel}\nabla_{\parallel} + (\boldsymbol{v}_{\mathrm{d}} + \boldsymbol{v}_{\mathrm{E}}) \cdot \nabla + \frac{e_{\alpha}}{m_{\alpha}}(v_{\parallel}E_{\parallel} + \boldsymbol{v}_{\mathrm{d}} \cdot \boldsymbol{E})\frac{\partial}{\partial \varepsilon}\right] f_{\alpha} = 0$$

- **Eigenvalue problem** for complex wave frequency
  - **Maximize wave amplitude** for finite excitation proportional to n_{e}

Coordinates

- **Magnetic Surface Coordinates** **(Non-Orthogonal)**
  - Minor radius direction:
    Poloidal Magnetic Flux ψ
  - Poloidal direction: θ
  - Toroidal direction: φ

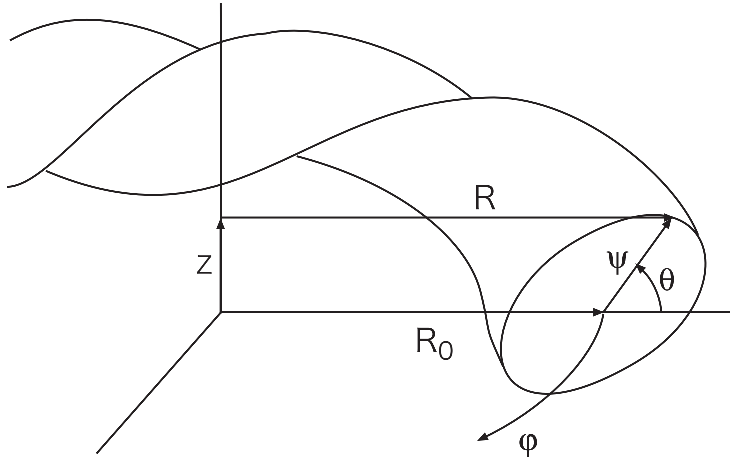

- **Co-variant expression** of $\boldsymbol{E}$

$$\boldsymbol{E} = E_1\boldsymbol{e}^1 + E_2\boldsymbol{e}^2 + E_3\boldsymbol{e}^3$$

where contra-variant basis

$$\boldsymbol{e}^1 = \boldsymbol{\nabla}\psi, \qquad \boldsymbol{e}^2 = \boldsymbol{\nabla}\theta, \qquad \boldsymbol{e}^3 = \boldsymbol{\nabla}\varphi$$

- J **: Jacobian** $\quad J = \dfrac{1}{\boldsymbol{e}^1 \cdot \boldsymbol{e}^2 \times \boldsymbol{e}^3} = \dfrac{1}{\boldsymbol{\nabla}\psi \cdot \boldsymbol{\nabla}\theta \times \boldsymbol{\nabla}\varphi}$

- g **: Metric tensor** $\quad g_{ij} = \boldsymbol{e}_i \cdot \boldsymbol{e}_j$, where co-variant basis $\boldsymbol{e}_i \equiv \partial \boldsymbol{r}/\partial x_i$

Wave Equation

- **Maxwell's equation** for stationary wave electric field $\boldsymbol{E}$ (angular frequency ω, light velocity c)

$$\nabla \times \nabla \times \boldsymbol{E} = \frac{\omega^2}{c^2} \overleftrightarrow{\epsilon} \cdot \boldsymbol{E} + \mathrm{i}\,\omega\mu_0 \boldsymbol{j}_{\mathrm{ext}}$$

  – $\overleftrightarrow{\epsilon}$ **: Dielectric tensor** : plasma response
    Cyclotron damping, Landau damping
  – $\boldsymbol{j}_{\mathrm{ext}}$: Antenna Current

- **Wave equation in non-orthogonal coordinates** (radial components)

$$(\nabla \times \nabla \times \boldsymbol{E})^1 = \frac{1}{J}\left[\frac{\partial}{\partial x^2}\left\{\frac{g_{31}}{J}\left(\frac{\partial E_3}{\partial x^2} - \frac{\partial E_2}{\partial x^3}\right) + \frac{g_{32}}{J}\left(\frac{\partial E_1}{\partial x^3} - \frac{\partial E_3}{\partial x^1}\right) + \frac{g_{33}}{J}\left(\frac{\partial E_2}{\partial x^1} - \frac{\partial E_1}{\partial x^2}\right)\right\}\right.$$
$$\left. - \frac{\partial}{\partial x^3}\left\{\frac{g_{21}}{J}\left(\frac{\partial E_3}{\partial x^2} - \frac{\partial E_2}{\partial x^3}\right) + \frac{g_{22}}{J}\left(\frac{\partial E_1}{\partial x^3} - \frac{\partial E_3}{\partial x^1}\right) + \frac{g_{23}}{J}\left(\frac{\partial E_2}{\partial x^1} - \frac{\partial E_1}{\partial x^2}\right)\right\}\right]$$

  – $(x^1, x^2, x^3) = (\psi, \theta, \varphi)$
  – Similar expression for poloidal and toroidal components

Response of Plasmas

- Usually the dielectric tensor $\overleftrightarrow{\epsilon}$ is calculated in Cartesian coordinates with static magnetic field along the z axis.
- **Local normalized orthogonal coordinates**

$$\hat{\boldsymbol{e}}_s = \frac{\boldsymbol{\nabla}\psi}{|\boldsymbol{\nabla}\psi|}, \quad \hat{\boldsymbol{e}}_b = \hat{\boldsymbol{e}}_h \times \hat{\boldsymbol{e}}_\psi, \quad \hat{\boldsymbol{e}}_h = \frac{\boldsymbol{B}_0}{|\boldsymbol{B}_0|}$$

- Variable Transformation: $\overleftrightarrow{\mu}$

$$\begin{pmatrix} E_1 \\ E_2 \\ E_3 \end{pmatrix} = \overleftrightarrow{\mu} \cdot \begin{pmatrix} E_s \\ E_b \\ E_h \end{pmatrix}$$

$$\overleftrightarrow{\mu} \equiv \begin{pmatrix} \dfrac{1}{\sqrt{g^{11}}} & \dfrac{d}{\sqrt{Jg^{11}}} & c_2 g_{12} + c_3 g_{13} \\ 0 & c_3 J\sqrt{g^{11}} & c_2 g_{22} + c_3 g_{23} \\ 0 & -c_2 J\sqrt{g^{11}} & c_2 g_{32} + c_3 g_{33} \end{pmatrix}$$

$$\begin{aligned} & c_2 = B^\theta / B, \quad c_2 = B^\phi / B \\ & d = c_2(g_{23}g_{12} - g_{22}g_{31}) + c_3(g_{33}g_{12} - g_{32}g_{31}) \\ & g^{11} = (g_{22}g_{33} - g_{23}g_{32})/J^2 \end{aligned}$$

- **Dielectric tensor in non-orthogonal coordinates**:

$$\boxed{\overleftrightarrow{\epsilon} = \overleftrightarrow{\mu} \cdot \overleftrightarrow{\epsilon}_{sbh} \cdot \overleftrightarrow{\mu}^{-1}}$$

Fourier Mode Expansion

- **Fourier expansion in poloidal and toroidal directions**
- Spatial variation of wave electric field, medium and the L.H.S. of Maxwell's equation

$$E(\psi,\theta,\varphi)=\sum_{mn}E_{mn}(\psi)e^{\mathrm{i}(m\theta+n\varphi)}$$

$$G(\psi,\theta,\varphi)=\sum_{lk}G_{lk}(\psi)e^{\mathrm{i}(l\theta+kN_p\varphi)}$$

$$J(\nabla\times\nabla\times\boldsymbol{E})=G(\psi,\theta,\varphi)E(\psi,\theta,\varphi)=\sum_{m'n'}[J(\nabla\times\nabla\times\boldsymbol{E})]_{m'n'}e^{\mathrm{i}(m'\theta+n'\varphi)}$$

- **Coupling between various modes** (N_h : Rotation number of helical coil in φ)

Mode Number	Toroidal Direcition	Poloidal Direction
Wave electric field $\boldsymbol{E}$	n	m
Medium G	kN_h	l
$J(\nabla\times\nabla\times\boldsymbol{E})$	n'	m'
Relations	$n'=n+kN_\mathrm{h}$	$m'=m+l$

Parallel Wave Number

- **Dielectric tensor** $\overleftrightarrow{\epsilon}(\psi, \theta, \varphi, k_{\parallel}^{m''n''})$ depends on parallel wave number $k_{\parallel}^{m'',n''}$ through the **plasma dispersion function** $Z[(\omega - N\omega_{\mathrm{cs}})/k_{\parallel}^{m''n''} v_{\mathrm{Ts}}]$

$$k_{\parallel}^{m'',n''} = -i\hat{\boldsymbol{e}}_h \cdot \boldsymbol{\nabla} = -i\hat{\boldsymbol{e}}_h \cdot (\boldsymbol{\nabla}\theta \frac{\partial}{\partial\theta} + \boldsymbol{\nabla}\varphi \frac{\partial}{\partial\varphi})$$

$$= -i\hat{\boldsymbol{e}}_h \cdot (\boldsymbol{e}^2 \frac{\partial}{\partial\theta} + \boldsymbol{e}^3 \frac{\partial}{\partial\varphi}) = m'' \frac{B^\theta}{|B|} + n'' \frac{B^\varphi}{|B|}$$

- **Fourier components of electric displacement**

$$\begin{array}{ccccccccc} (J\overleftrightarrow{\epsilon} \cdot \boldsymbol{E})^i & = & J\overleftrightarrow{g}^{-1} & \cdot \overleftrightarrow{\mu} & \cdot & \overleftrightarrow{\epsilon}_{sbh} & \cdot \overleftrightarrow{\mu}^{-1} & \cdot & \boldsymbol{E}_i \\ m' & & & \ell_3 & & \ell_2 & \ell_1 & & m \\ n' & & & k_3 & & k_2 & k_1 & & n \end{array}$$

therefore

$$m'' = m + \ell_1 + \frac{1}{2}\ell_2 \qquad n'' = n + k_1 + \frac{1}{2}k_2$$

$$m' = m + \ell_1 + \ell_2 + \ell_2 \qquad n' = n + k_1 + k_2 + k_3$$

Destabilization by Energetic Ion

- **Drift kinetic equation**

$$\left[\frac{\partial}{\partial t} + v_{\|}\nabla_{\|} + (\boldsymbol{v}_{\rm d} + \boldsymbol{v}_{\rm E})\cdot\boldsymbol{\nabla} + \frac{e_\alpha}{m_\alpha}(v_{\|}E_{\|} + \boldsymbol{v}_{\rm d}\cdot\boldsymbol{E})\frac{\partial}{\partial\varepsilon}\right] f_\alpha = 0$$

where

$$\varepsilon = \frac{1}{2}m_\alpha v^2, \quad \boldsymbol{v}_{\rm E} = \frac{\boldsymbol{E}\times\boldsymbol{B}}{B^2}, \quad \boldsymbol{v}_{\rm d} = v_{\rm d}\sin\theta\hat{\boldsymbol{r}} + v_{\rm d}\cos\theta\hat{\boldsymbol{\theta}},$$

$$v_{\rm d} = \frac{m_\alpha}{e_\alpha BR}\cdot\frac{v_\perp^2}{v_\perp^2 + v_{\|}^2}$$

- **Linear response**
  - Velocity integral of perturbed distribution function
  - Poloidal mode coupling due to magnetic drift motion

Response of Energetic Particles

- **Anti-Hermite part of electric susceptibility tensor**

$$\overleftrightarrow{\chi}_{mm'} = \begin{pmatrix} 1 & -\mathrm{i} & 0 \\ -\mathrm{i} & -1 & 0 \\ 0 & 0 & 0 \end{pmatrix} P_{m-1,m-2}\delta_{m',m-2} + \begin{pmatrix} 0 & 0 & Q_{m-1,m-1} \\ 0 & 0 & -\mathrm{i}\,Q_{m-1,m-1} \\ Q_{m,m-1} & -\mathrm{i}\,Q_{m,m-1} & 0 \end{pmatrix} \delta_{m',m-1}$$

$$+ \begin{pmatrix} (P_{m-1,m} + P_{m+1,m}) & \mathrm{i}\,(P_{m-1,m} - P_{m+1,m}) & 0 \\ -\mathrm{i}\,(P_{m-1,m} - P_{m+1,m}) & (P_{m-1,m} + P_{m+1,m}) & 0 \\ 0 & 0 & R_{m-1,m-1} \end{pmatrix} \delta_{m',m}$$

$$+ \begin{pmatrix} 0 & 0 & Q_{m+1,m+1} \\ 0 & 0 & \mathrm{i}\,Q_{m+1,m+1} \\ Q_{m,m+1} & \mathrm{i}\,Q_{m,m+1} & 0 \end{pmatrix} \delta_{m',m+1} + \begin{pmatrix} 1 & \mathrm{i} & 0 \\ \mathrm{i} & -1 & 0 \\ 0 & 0 & 0 \end{pmatrix} P_{m+1,m+2}\delta_{m',m+2}$$

- **In the case of Maxwellian velocity distribution**

$$P_{m,m'} = \mathrm{i}\,\frac{\omega_{\mathrm{p}\alpha}^2}{2\omega^2}\left(1 - \frac{\omega_{*\alpha m'}}{\omega}\right)\frac{\rho_\alpha^2}{R^2}\sqrt{\pi}x_m\left(\frac{1}{2} + x_m^2 + x_m^4\right)\mathrm{e}^{-x_m^2}$$

$$Q_{m,m'} = \mathrm{i}\,\frac{\omega_{\mathrm{p}\alpha}^2}{2\omega^2}\left(1 - \frac{\omega_{*\alpha m'}}{\omega}\right)\frac{\rho_\alpha}{R}\sqrt{\pi}2x_m^2\left(\frac{1}{2} + x_m^2\right)\mathrm{e}^{-x_m^2}$$

$$R_{m,m'} = \mathrm{i}\,\frac{\omega_{\mathrm{p}\alpha}^2}{2\omega^2}\left(1 - \frac{\omega_{*\alpha m'}}{\omega}\right)\sqrt{\pi}4x_m^3\mathrm{e}^{-x_m^2}$$

$$x_m = \omega/|k_{\parallel m}|v_{\mathrm{T}\alpha}, \qquad \rho_\alpha = v_{\mathrm{T}\alpha}/\omega_{\mathrm{c}\alpha}, \qquad v_{\mathrm{T}\alpha} = \sqrt{2T_\alpha/m_\alpha}$$

Boundary Conditions

- Calculation region surrounded by **perfectly conducting wall** (**Vacuum region** exists between plasma surface and wall)
- Boundary condition on the conducting wall:
  Tangential components of $\boldsymbol{E}$ vanishes.
  - Co-variant expression ($\boldsymbol{E} = E_1 \nabla\psi + E_2 \nabla\theta + E_3 \nabla\varphi$): $E_2 = 0$, $E_3 = 0$
- Boundary condition on the magnetic axis ($\psi = 0$):
  Finiteness of the wave magnetic field and the induced charge density

$$\begin{cases} m = 0 & \dfrac{\partial E_\varphi^{0n}}{\partial \psi} = 0 \\ m \neq 0 & E_\varphi^{mn} = 0 \end{cases}$$

Co-variant component E_θ^{mn} always vanishes on the axis.

Typical TAE with Positive Magnetic Shear

- **Configuration**
  - $q(\rho) = q_0 + (q_a - q_0)\rho^2,\ q_0 = 1,\ q_a = 2$
  - Flat Density Profile

Alfvén Frequency

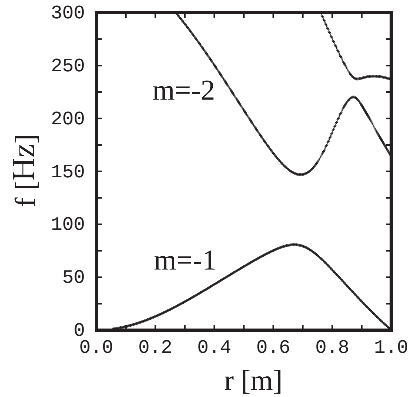

Contour of $|E|^2$ in Complex Frequency Space

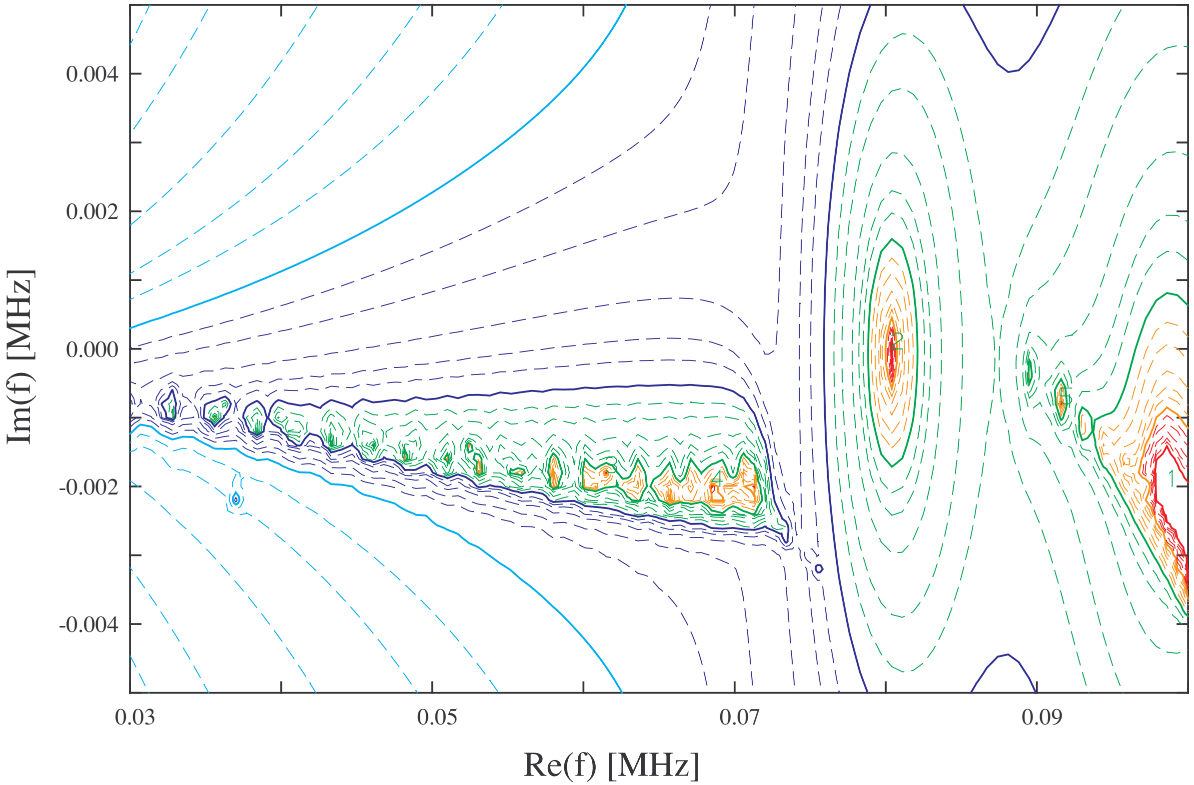

Eigen function

$$f_r = 81.95\,\text{kHz}$$
$$f_i = -20.32\,\text{Hz}$$

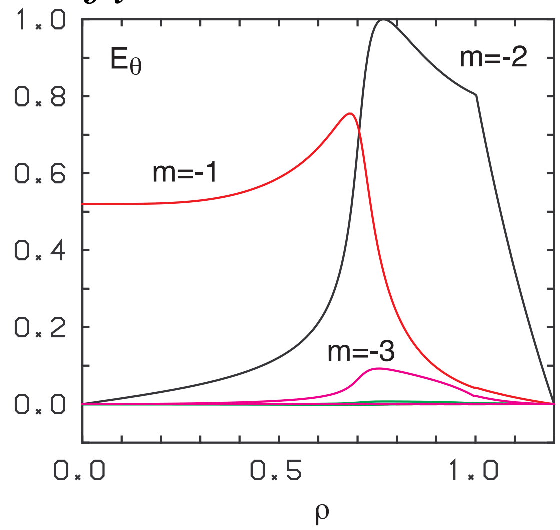

Energetic Particle Mode (EPM)

- Energetic ions can excite EPM with frequency below the TAE frequency gap.
- With β of energetic ions about 0.5%, ω_A and contour of wave amplitude

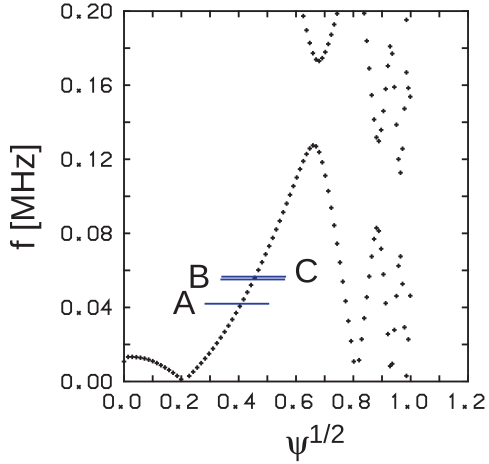

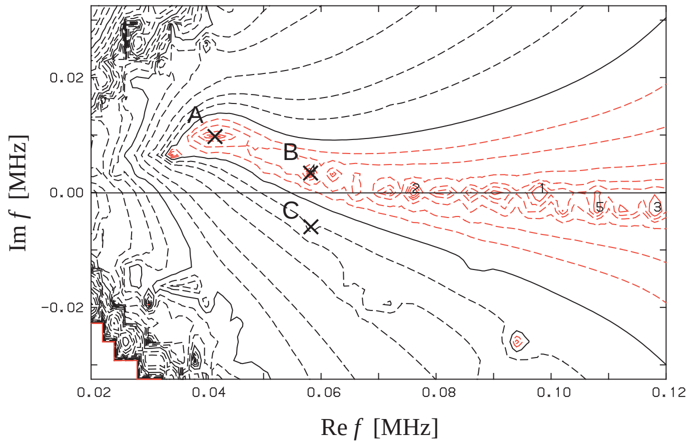

- Eigenmode structure

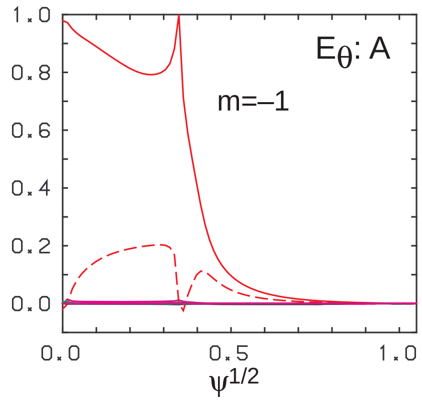

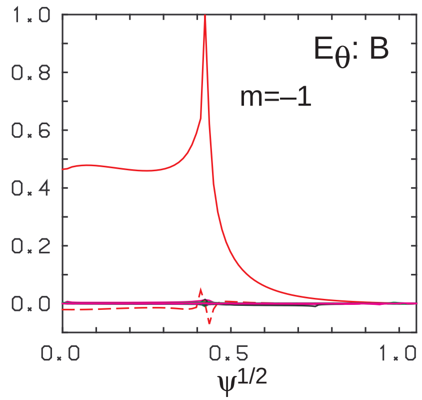

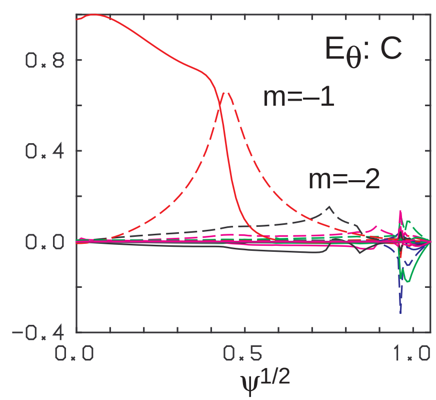

A: $f_r = 41.8\,\text{kHz}$ B: $f_r = 57.7\,\text{kHz}$ C: $f_r = 58.0\,\text{kHz}$

A: $f_i = 8.1\,\text{kHz}$ B: $f_i = 3.6\,\text{kHz}$ C: $f_i = -6.0\,\text{kHz}$

Parameter Dependence of Mode Structure

$n_{F0} = 0 \times 10^{17}\,\mathrm{m}^{-3}$, $T_B = 0.5\,\mathrm{MeV}$

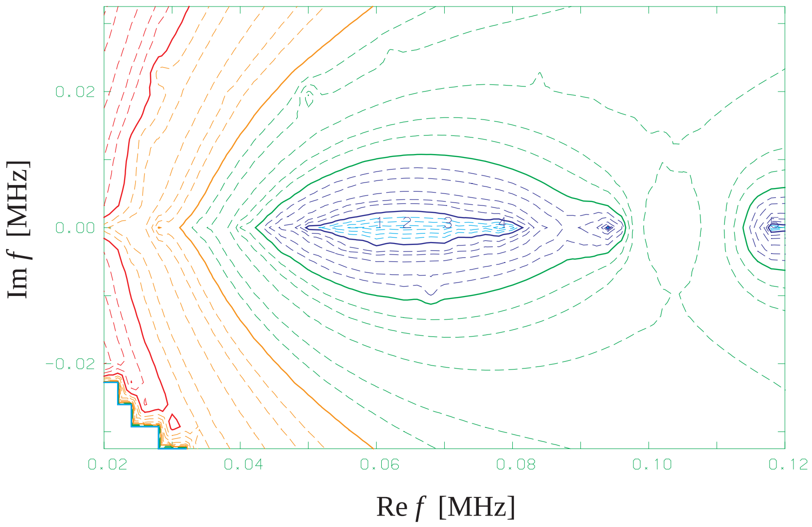

$n_{F0} = 1 \times 10^{17}\,\mathrm{m}^{-3}$, $T_B = 0.5\,\mathrm{MeV}$

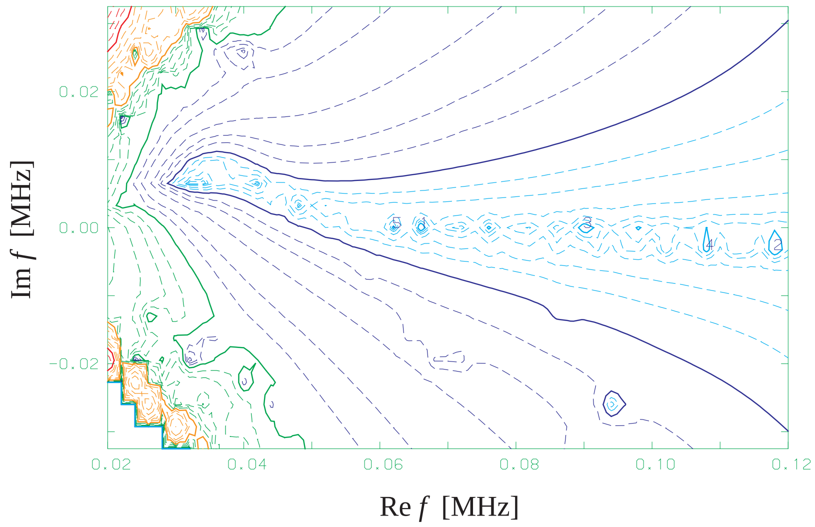

$n_{F0} = 3 \times 10^{17}\,\mathrm{m}^{-3}$, $T_B = 0.5\,\mathrm{MeV}$

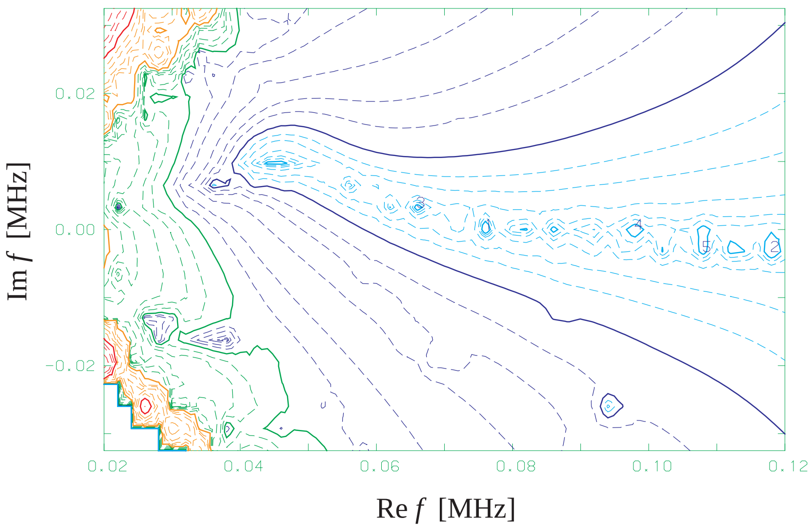

$n_{F0} = 1 \times 10^{17}\,\mathrm{m}^{-3}$, $T_B = 1\,\mathrm{MeV}$

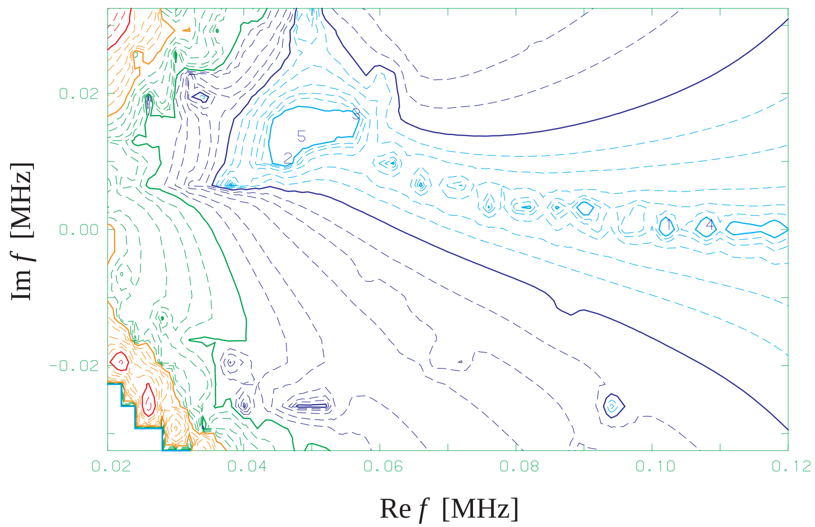

Effect of Toroidal Plasma Rotation

Experimental Results on JT-60U

Ref. M. Saigusa et al., Nucl. Fusion, 37 (1997) 1559.

Co-NBI ⟶ Counter-NBI	**Counter-NBI ⟶ Co-NBI**

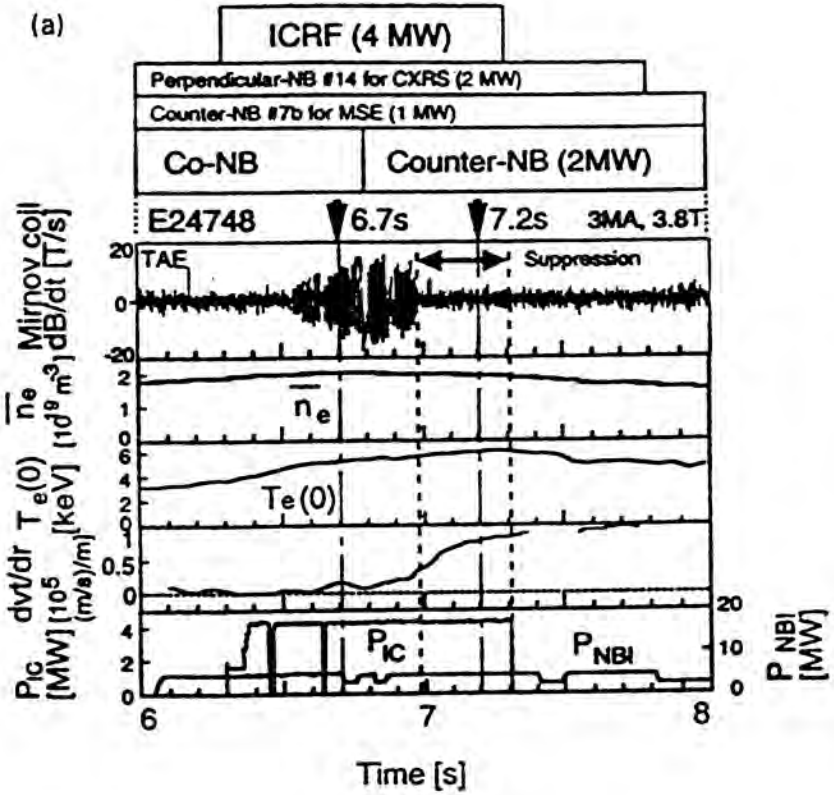

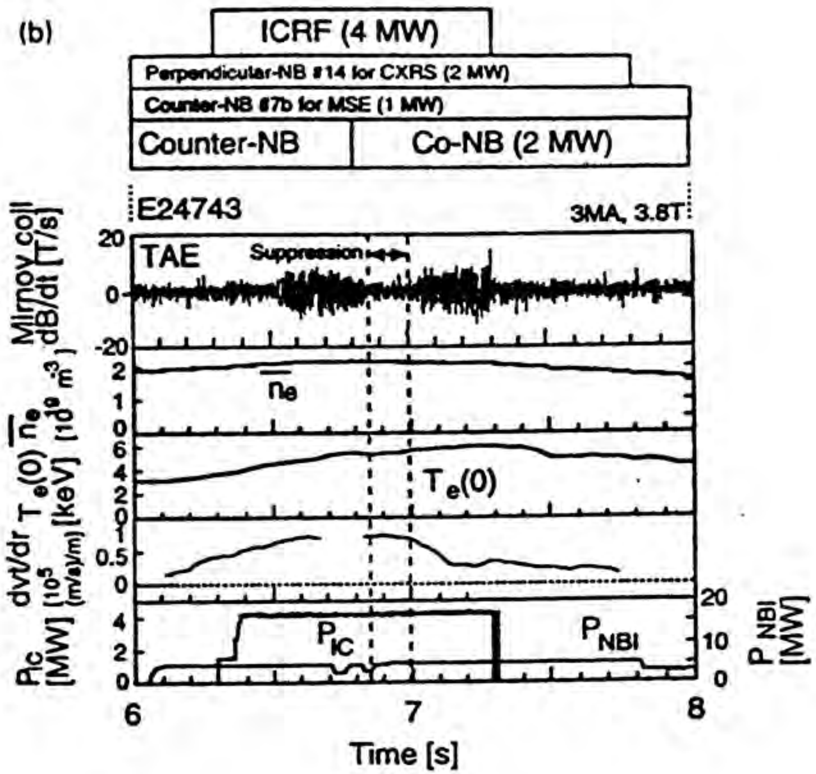

Counter-NBI: stabilization	Co-NBI: destabilization

Dispersion Relation including Toroidal Rotation

- **Dispersion relation**

$$\left({k_{\|m}}^2 - \frac{(\omega - k_{\|m}u)^2}{{v_\mathrm{A}}^2}\right)\left({k_{\|m+1}}^2 - \frac{(\omega - k_{\|m+1}u)^2}{{v_\mathrm{A}}^2}\right) - \epsilon^2\frac{(\omega - k_{\|m}u)^2(\omega - k_{\|m+1}u)^2}{{v_\mathrm{A}}^4} = 0$$

- Parallel wave number @$k_{\|m} = \dfrac{1}{R}\left(n + \dfrac{m}{q}\right)$
- Alfvén resonance condition without toroidal effect

$$\omega^2 = {k_{\|m}}^2(u \pm v_\mathrm{A})^2, \qquad \omega^2 = {k_{\|m+1}}^2(u \pm v_\mathrm{A})^2$$

- Condition for frequency gap

$$k_{\|m}\left(u - v_\mathrm{A}\right) = k_{\|m+1}\left(u + v_\mathrm{A}\right)$$

- **Safety factor at TAE gap**: q

$$q = -\frac{m + 1/2}{n} - \frac{1}{2n}\frac{u}{v_\mathrm{A}}$$

- **TAE gap frequency** ω: parabolic with respect to u

$$\omega = \frac{v_\mathrm{A}}{2qR}\left(1 - \frac{u^2}{{v_\mathrm{A}}^2}\right)$$

Effect of Rotation on $n = 1$ mode

$n = 1$ Eigenmode for JT-60U parameters

$E_{\theta m}$

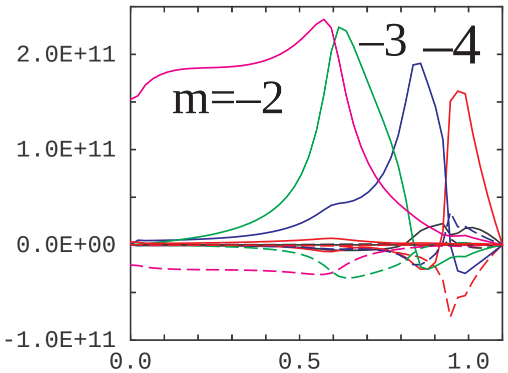

$|E_{\theta m}|$

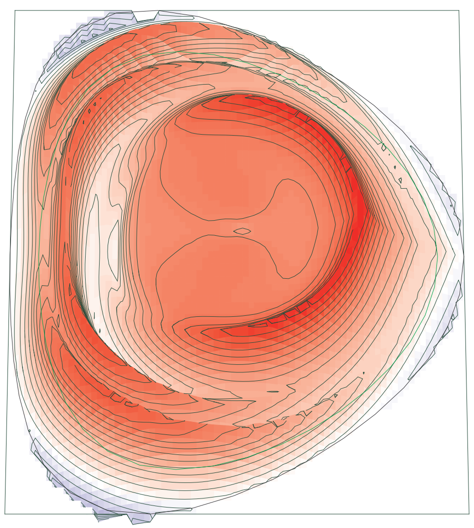

Dependence of eigen frequency and damping rate on

Rotation Velocity

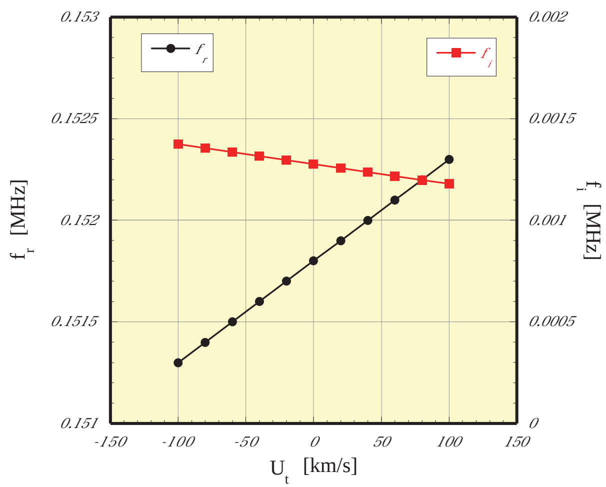

Velocity Gradient

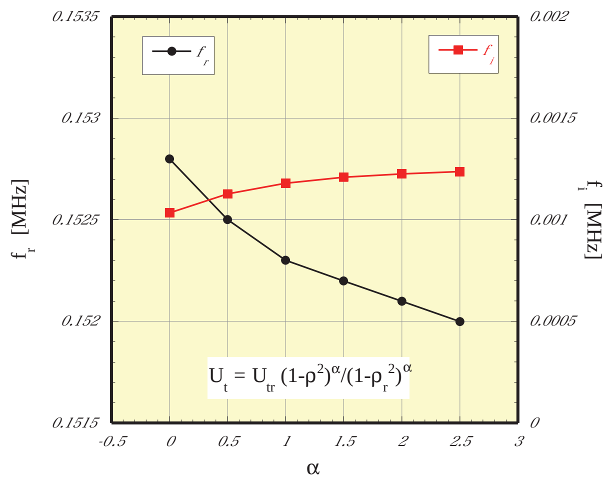

Effect of Rotation on $n = 7$ mode

- Ref. M. Saigusa et al., Nucl. Fusion **37** (1997) 1559.
- $n = 7, m = -17 \sim -3, f = 223\,\mathrm{kHz}$ Good agreement with Nova-K

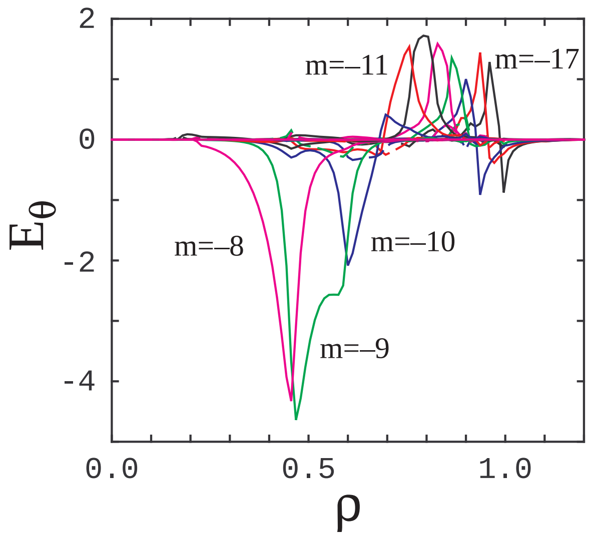

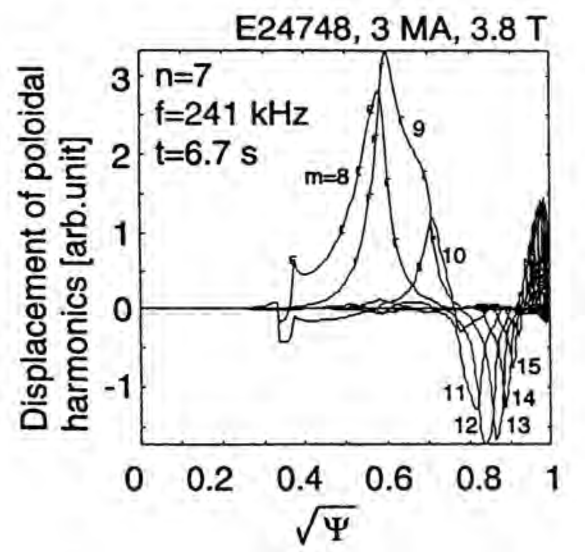

- Rotation velocity dependence: Stabilizing for co rotation (Contradict with exp.)

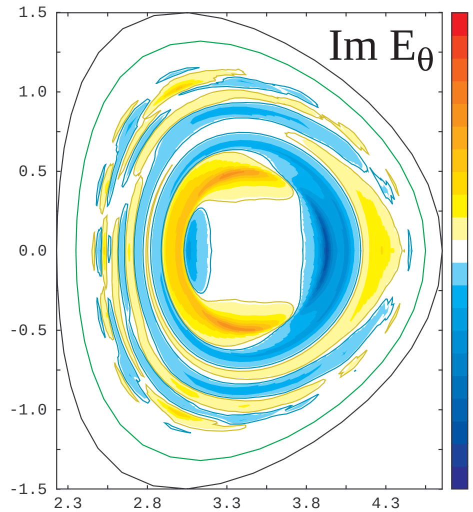

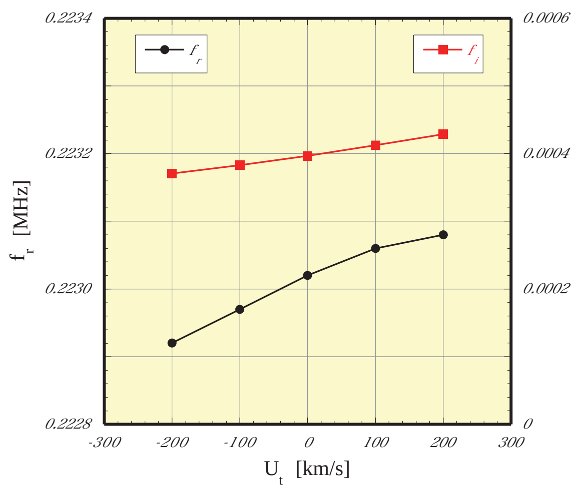

Influence of poloidal mode range : $n = 7$ mode

- Radial structure of Alfvén Continuum

$m = -17 \sim -3$

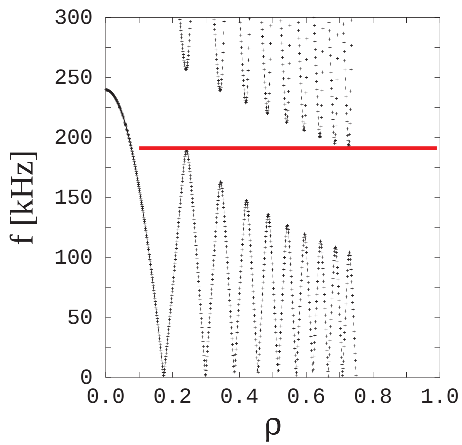

$m = -21 \sim -7$

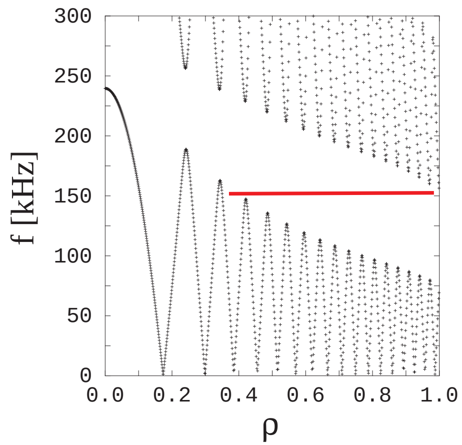

- $n = 7, m = -21 \sim -7, f = 238\,\mathrm{kHz}$FDestabilizing for co-rotation (agree with exp.)

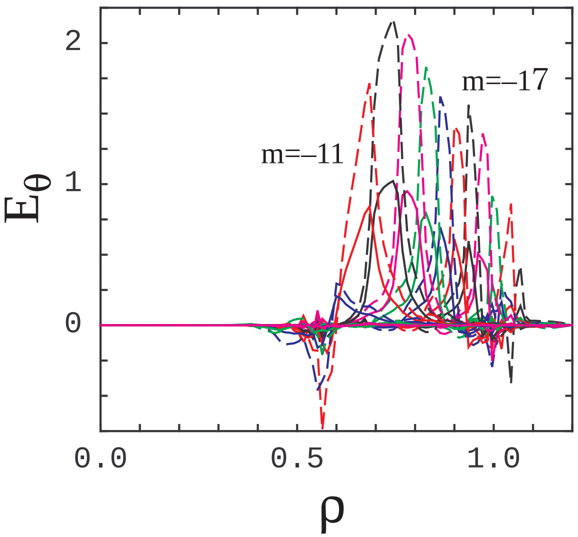

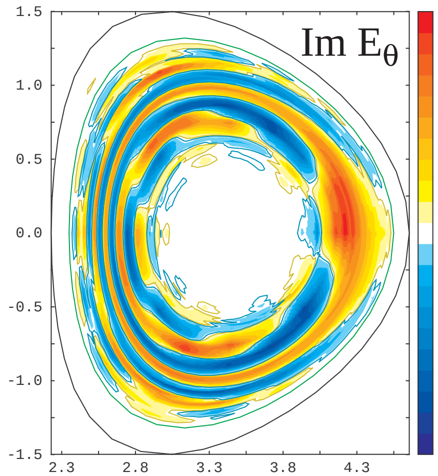

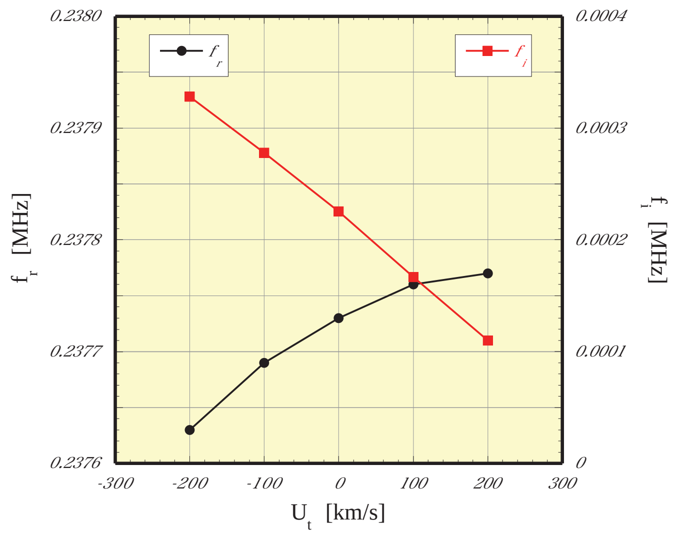

AE in the Reversed Magnetic Shear Configuration (JT-60U)

- Takechi et al. IAEA 2002 (Lyon) EX/W-6

Fluctuation Amplitude

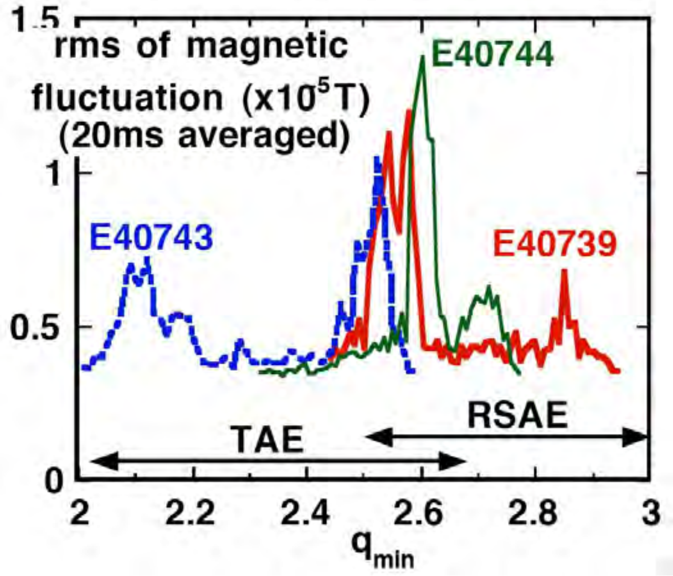

Observed frequency **calculated frequency**

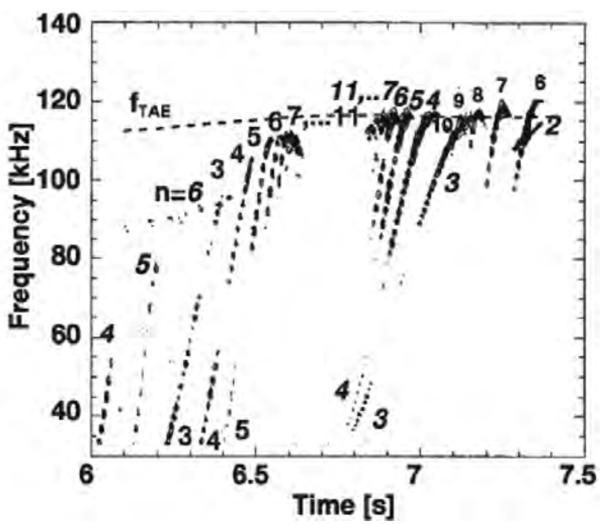

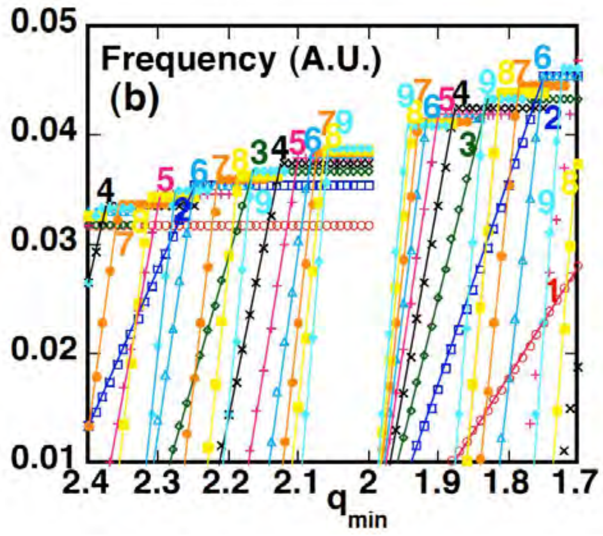

First observation of RSAE by TASK/WM

- Analysis of AE in RS Configuration at TCM on EP in 1997.

IAEA Technical Committee Meeting on
Alpha-Particles in Fusion Research
September 8–11, 1997
JET, Abington, UK

Kinetic Analysis of TAE in Tokamaks and Helical Devices

A. Fukuyama and T. Tohnai

Faculty of Engineering, Okayama University, Okayai

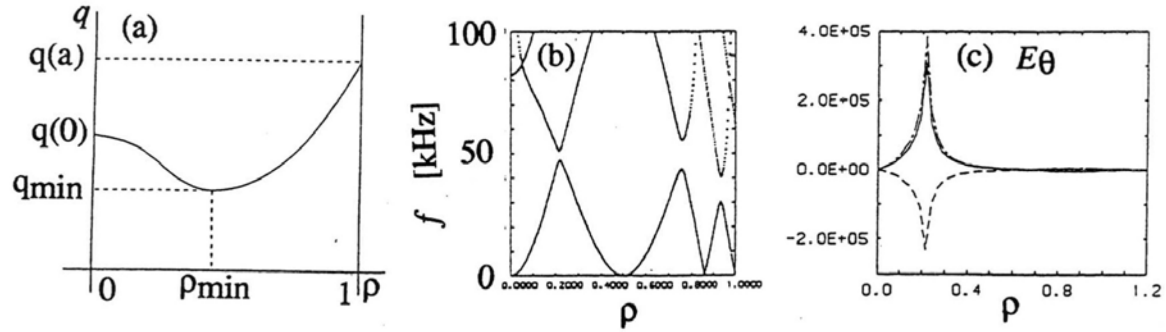

Fig.4: Radial profile of q (a), resonance frequency (b) and eigen function (c) in the case of negative shear; $q(0)=3$, $q_{\min}=2$, $q(a)=5$ *and* $n=1$.

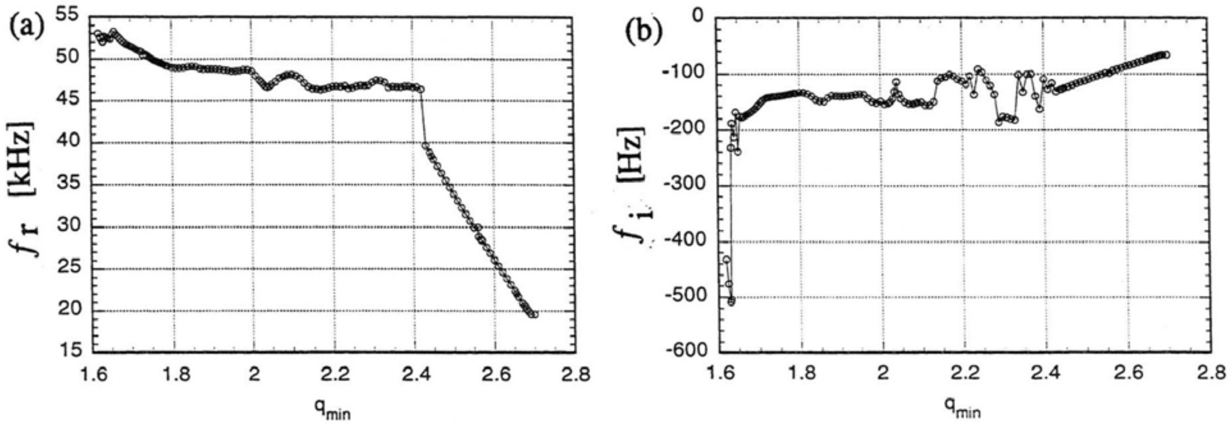

Fig.5: $q_{\min}$ *dependence of the eigen frequency; real part (a) and imaginary part (b)*

Analysis of AE in Reversed Shear Configuration

Assumed q profile

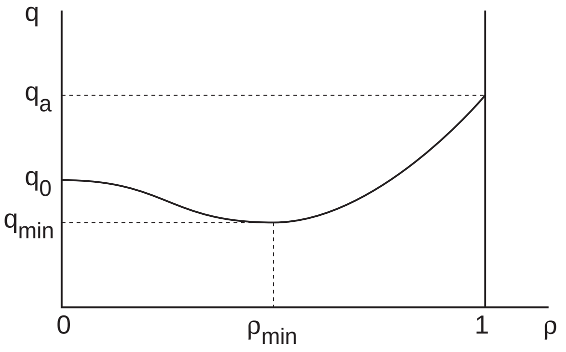

Plasma Parameters

R_0	3 m
a	1 m
B_0	3 T
$n_e(0)$	$10^{20}\,\mathrm{m}^{-3}$
$T(0)$	3 keV
$q(0)$	3
$q(a)$	5
$\rho_{\min}$	0.5
n	1

Flat density profile

$q_{\min}$ Dependence of Eigenmode Frequency

Real part

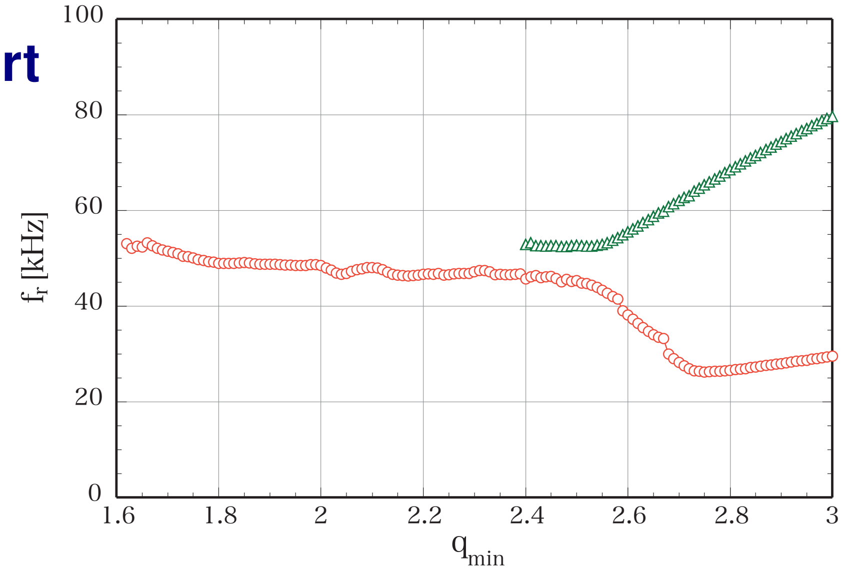

Imag part

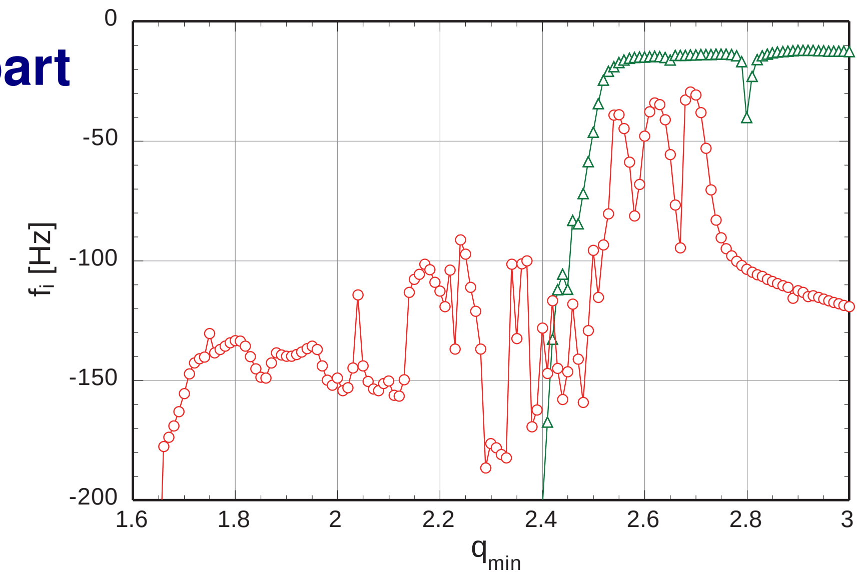

- **RSAE (reversed-shear-induced Alfvén eigenmode)** for $\ell + \frac{1}{2} < q_{\min} < \ell + 1$

q_{min} Dependence of Radial Structure of Alfvén resonance

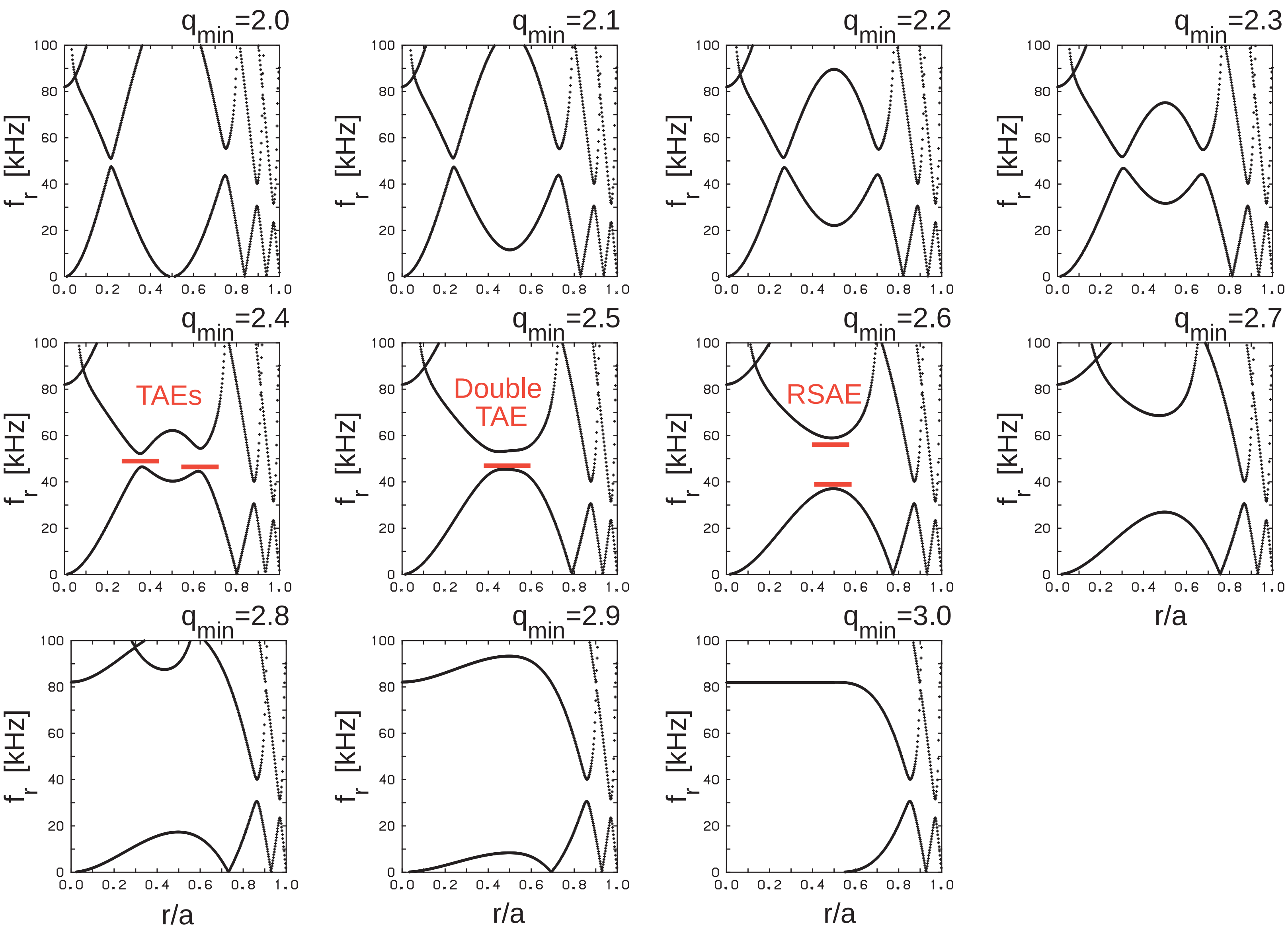

Eigenmode Structure ($n = 1$)

$q_{\min} = 2.4$ | $q_{\min} = 2.5$ | $q_{\min} = 2.6$

Alfvén resonance

Higher freq.

Lower freq.

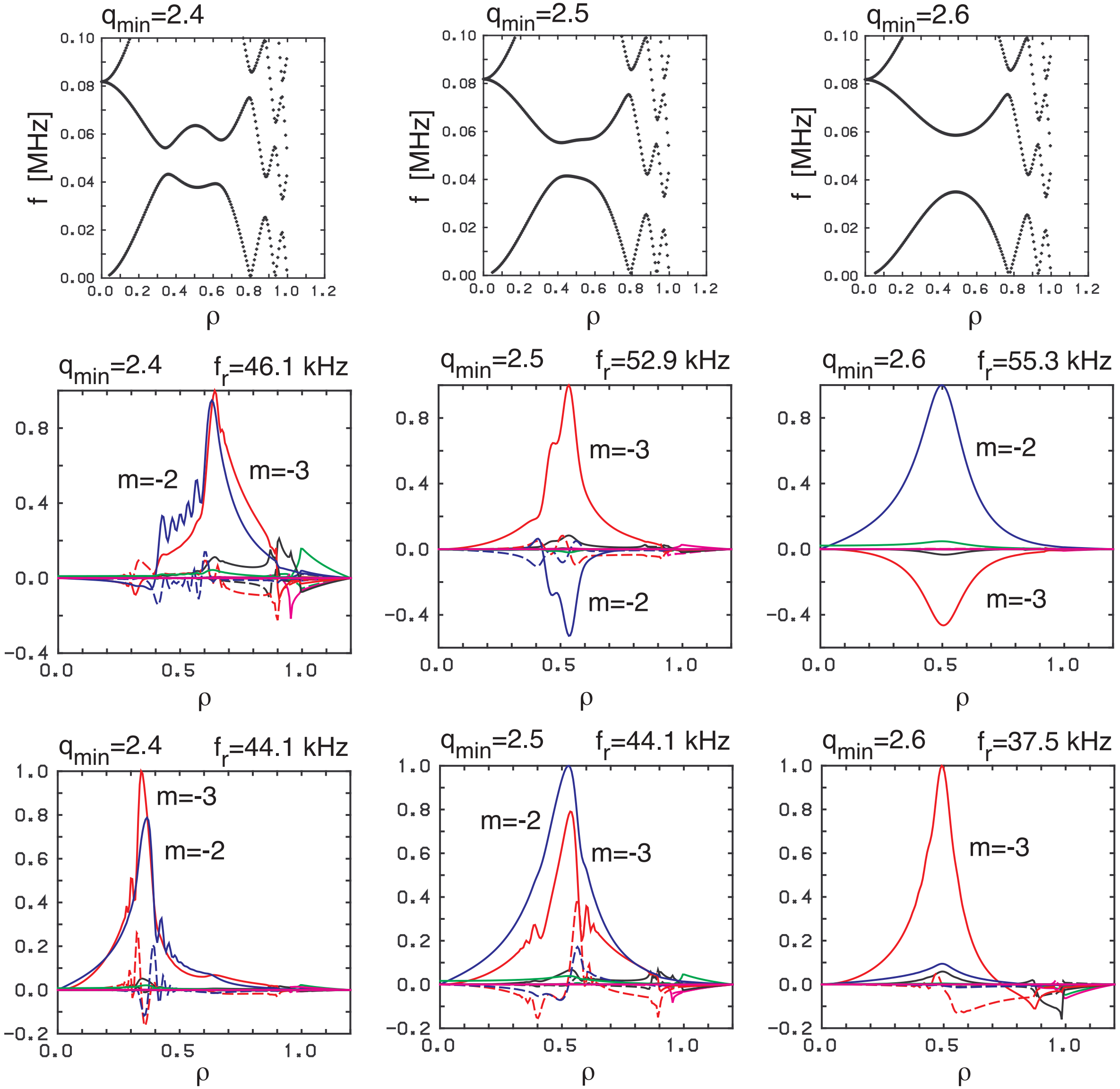

TAEs | **Double TAE** | **RSAE**

Excitation by Energetic Particles ($q_{\min} = 2.6$)

- Without EP

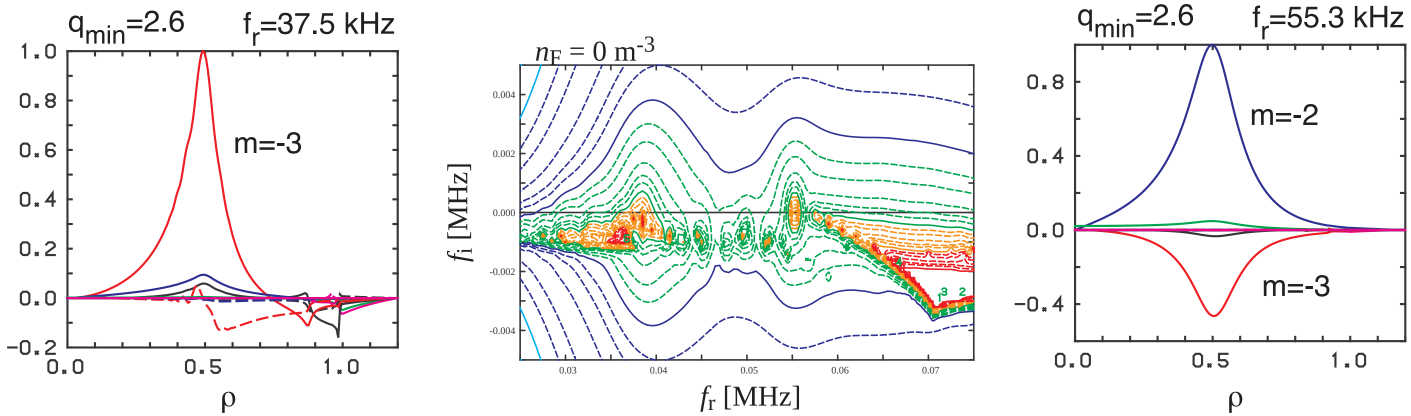

- With EP

  $3 \times 10^{16}\,\mathrm{m}^{-3}$
  360 keV
  0.5 m

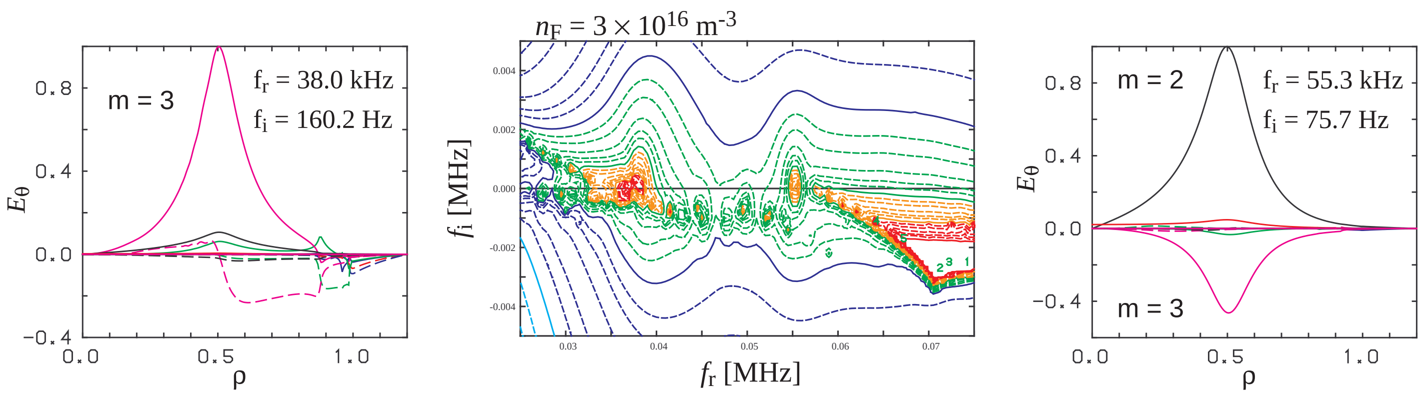

- With EP

  $1 \times 10^{17}\,\mathrm{m}^{-3}$
  360 keV
  0.5 m

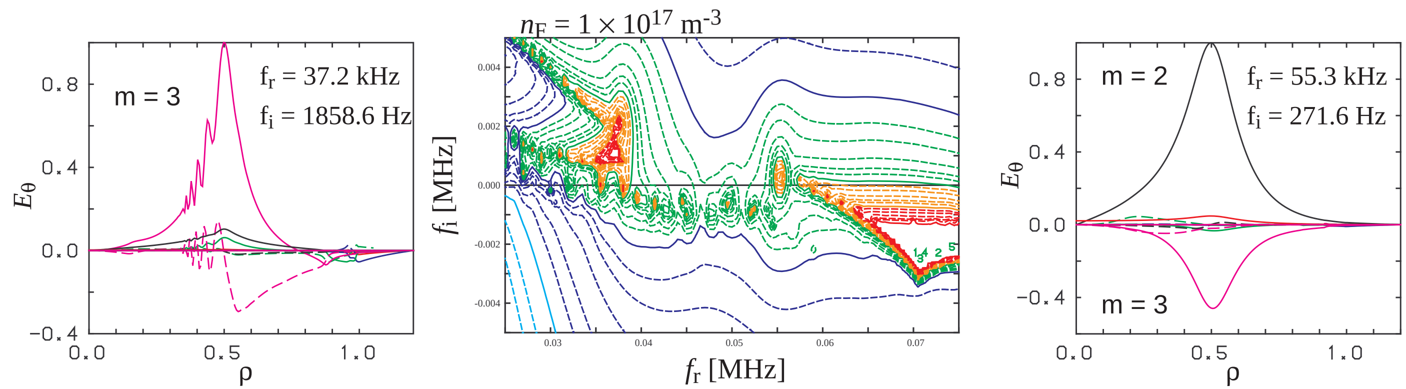

Progress in Full Wave Analysis

- **Variety of numerical schemes**

module	system	scheme
WM	torus	toroidal & poloidal: FFT, radial: FDM
WMF	torus	toroidal & poloidal: FFT, radial: FEM
WF2D	torus	toroidal: FFT, poloidal and radial: FEM
WF3D	Cartesian	x, y, z: FEM

  – Merit of FEM: Flexibility of mesh, sparse matrix, localized analysis

- **Extension of dielectric tensor**
  – Uniform, kinetic, Maxwellian, Fourier expansion
  – Nonuniform, gyro kinetic, Maxwellian, Fourier expansion
  – Nonuniform, kinetic, Maxwellian, Integral form
  – Uniform, kinetic, arbitrary $f(\boldsymbol{v})$, Fourier expansion
  – Nonuniform, gyro kinetic, arbitrary $f(\boldsymbol{v})$, Fourier expansion

- **Coupling with Fokker-Planck analysis of $f(\boldsymbol{v})$**

Momentum Distribution Functions

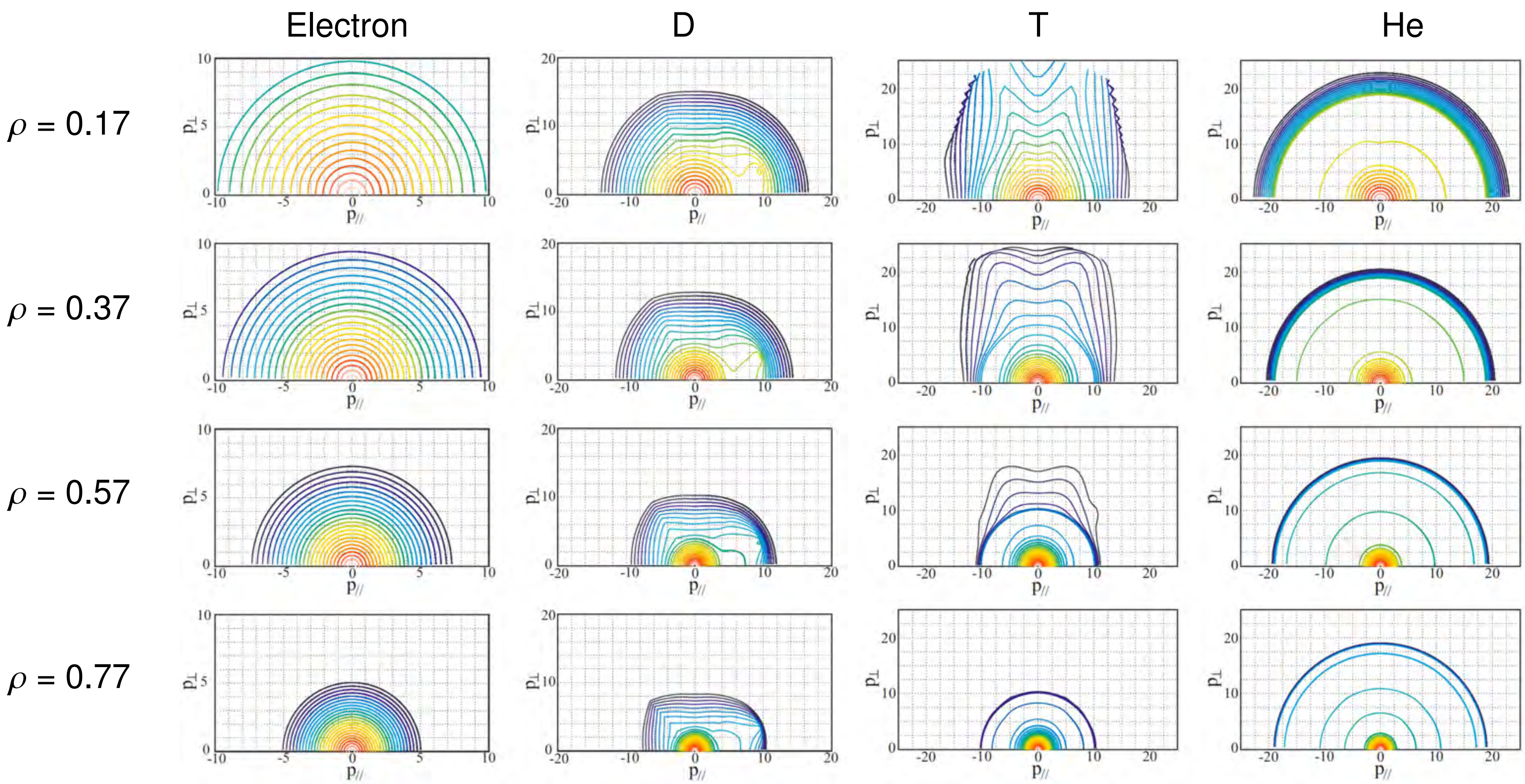

- **Radial diffusion proportional to $E^{-1/2}$ reduces energetic ions in the outer region.**

Summary

- Full wave approach of linear stability analysis is powerful for systematic analysis of various kinds of global eigenmodes.
  - Alfvén eigenmodes
  - Resistive wall mode, internal kink mode, $\cdots$
- Kinetic effects of energetic particles and bulk species can be included in the dielectric tensor, though non-uniformity and gyrokinetic effects may complicate the derivation.
- A variety of Alfvén eigenmodes have been analyzed by TASK/WM and the results were compared with other codes and experimental observations.
- Large scale computer will enable us to carry out systematic parameter survey in more realistic plasma models for future reactors..